EEET ECOLOGICAL ENGINEERING & ENVIRONMENTAL TECHNOLOGY

Ecological Engineering & Environmental Technology, 2026, 27(9), 240–259
https://doi.org/10.12912/27197050/226339
ISSN 2719–7050, License CC-BY 4.0

Received: 2026.07.13
Accepted: 2026.08.03
Published: 2026.08.15

Reconstructed soil pore geometry reveals associations with soil organic carbon depletion and salinity variability in converted tropical coastal wetlands

I Gusti Ngurah Putu Dharmayasa[1*], Cindy Aulia Citra[1], Umbu Erens Ndawa Lu[1], Chica Rambu Kupang Renggi[1], I Putu Sugiana[2], Roberth Evander Meidudga[3]

[1] Department of Civil Engineering, Faculty of Engineering and Informatics, Universitas Pendidikan Nasional, Denpasar 80224, Indonesia
[2] Department of Aquatic Resources Management, Faculty of Agriculture, Science and Technology, Universitas Warmadewa, Denpasar 80235, Bali, Indonesia
[3] Department of Civil and Structural Engineering, University of Sheffield, Mappin Street, Sheffield, United Kingdom
* Corresponding author's e-mail: ngurahdharmayasa@undiknas.ac.id

ABSTRACT

Land-use conversion in tropical coastal wetlands profoundly alters sediment geotechnics and biogeochemistry, yet their complex interactions remain poorly integrated. This study evaluated the relationships among sediment pore geometry, soil organic carbon (SOC), and salinity (EC) across five distinct natural and anthropogenic land-cover types in southern Denpasar, Bali. This study integrates geotechnical pore geometry analysis with biogeochemical indicators across five contrasting coastal land-use types to evaluate how anthropogenic land-use conversion modifies sediment structure and ecosystem functioning. To ensure internally consistent estimates of pore geometry, established soil mechanics equations, including the theoretical mixture equation and conventional soil phase relationships, were applied within a reproducible analytical workflow. Data were evaluated using Kruskal-Wallis tests, Spearman correlations, and inverse distance weighting (IDW) spatial interpolation. Results demonstrated that pore geometry positively correlates with SOC ($r_s = 0.757$, $p = 0.001$). Anthropogenic land-use conversion, particularly to commercial aquaculture ponds, was consistently associated with reduced pore geometry and lower soil organic carbon (SOC), reflecting substantial deterioration of sediment structural condition across the investigated coastal wetland sites. This structural degradation significantly heightens land subsidence vulnerability and severely undermines the ecosystem's blue carbon sink capacity. Conversely, EC lacked correlation with pore geometry. IDW mapping visually confirmed that salinity is dictated by external hydrological forcing, evidenced by irrigation-driven salt leaching in paddy fields and toxic salinity anomalies in natural mangroves adjacent to a landfill. Sustainable coastal management necessitates an integrated spatial strategy to mitigate mechanical disturbances, protect blue carbon stores, and halt subsurface pollution.

Keyword: coastal wetlands, land-use conversion, pore geometry, organic carbon, salinity.

INTRODUCTION

Tropical coastal wetland ecosystems, encompassing mangrove forests, tidal marshes, and mudflats, are globally recognized as transitional environments with highly vital ecological functions. Hydrologically and biogeochemically, these areas act as natural buffers that protect the mainland from seawater intrusion, while simultaneously serving as highly efficient carbon sinks (He et al., 2025; James et al., 2024; Newton et al., 2020; Temmerman et al., 2023). However, driven by population growth and economic demands, coastal regions are currently facing massive anthropogenic pressures. The conversion of natural landscapes into built environments, aquaculture ponds, and paddy field has drastically altered the natural equilibrium of these ecosystems (Newton et al., 2020; Prasad, 2021; Saengsupavanich et al., 2024).

This condition is clear along the southern coast of Denpasar, Bali. As an area directly adjacent to rapid urbanization and tourism development, the southern coast of Denpasar exemplifies the dynamics of a tropical coastal region undergoing intensive land-cover transition (Christiawan and Nguyen, 2024; Rimba et al., 2020; Sunarta and Saifulloh, 2022). The conversion of mangrove habitats and mudflats into commercial aquaculture ponds and paddy fields not only alters the above-ground landscape but also fundamentally transforms the mechanical structure of the soil matrix and subsurface geochemical cycles (Lin et al., 2024; Yang et al., 2025). Furthermore, shifts in the hydrological regime and mechanical compaction processes during land-use conversion are believed to trigger the degradation of organic matter and alter the soil's capacity for salinity retention (Jha et al., 2023; Stagg et al., 2017).

Although the threats associated with land-use conversion have been extensively studied, the existing literature remains largely fragmented across separate scientific disciplines. The majority of ecological studies on coastal wetlands focus primarily on vegetation dynamics, biodiversity, or carbon stocks in isolation. Conversely, coastal geotechnical studies typically evaluate only the physical and mechanical index parameters of the soil such as bearing capacity and consolidation without linking these to broader ecosystem functions (Brown et al., 2021; Kaden et al., 2026; Li et al., 2018; Liu et al., 2025). Consequently, a significant research gap remains in correlating how mechanical interventions which alter physical soil parameters such as grain-size distribution, porosity, and void ratio directly govern fundamental biogeochemical parameters, particularly soil organic carbon (SOC) retention and salinity fluctuations (electrical conductivity/EC) (Alharbi, 2025; Meurer et al., 2020).

Therefore, this study aims to quantify the impacts of coastal land-cover transitions specifically the conversion of natural ecosystems (mangroves, mudflats, and marshes) into anthropogenic land uses (aquaculture ponds and paddy fields) on the interplay between the physical index and chemical properties of the soil. Utilizing the southern coast of Denpasar as a field laboratory, this study investigates how alterations in soil pore geometry (porosity and void ratio) govern the soil's capacity to retain organic matter and regulate salinity levels. The findings of this research are expected to provide baseline data and a foundational framework that bridges soil mechanics and biogeochemistry, ultimately supporting sustainable coastal zone management. We hypothesize that conversion to anthropogenic land uses reduces soil porosity, which in turn limits SOC retention and increases salinity accumulation due to impeded hydrological fluxes.

Previous studies have generally evaluated either the geotechnical properties or the biogeochemical characteristics of coastal sediments separately, leaving limited understanding of how these two domains interact under anthropogenic land-cover change. This study addresses this gap by integrating geotechnical pore geometry analysis with biogeochemical indicators within a unified analytical framework to evaluate how anthropogenic land-use change modifies sediment structure and associated soil functions across five contrasting coastal land-use types. The primary scientific contribution of this study lies in the interdisciplinary integration of established soil mechanics principles with biogeochemical assessment, rather than in the development of a new pore-geometry method. Rather than testing a previously established relationship in isolation, this study evaluates how reconstructed pore geometry parameters can be used as integrative indicators linking sediment physical condition with ecosystem functioning across contrasting coastal land-use types.

Accordingly, the reconstruction of pore geometry parameters (Gs, e, and n) is presented as a reproducible analytical workflow based on established soil mechanics equations. The objectives of this study are threefold: (1) to estimate physically consistent pore geometry parameters (G_s, ρ_d, e, and n) from routinely measured laboratory variables using established soil mechanics equations; (2) to evaluate the relationships between pore geometry parameters and key biogeochemical indicators, including soil organic carbon and EC, using non-parametric statistical analyses; and (3) to assess how anthropogenic land-cover conversion influences the physical and biogeochemical characteristics of coastal sediments in the southern coastal wetlands of Denpasar, Indonesia. Based on these objectives, it is hypothesized that anthropogenic land-cover conversion modifies sediment pore geometry, resulting in changes in organic carbon retention and salinity dynamics through alterations in sediment physical structure and associated hydrological conditions.

MATERIAL AND METHOD

This study was designed based on a conceptual framework that links anthropogenic land-cover change with modifications in sediment physical structure and associated biogeochemical responses. The framework summarizes the hypothesized relationships among the investigated variables and provides the basis for the analytical approach adopted in this study, as illustrated in Figure 1.

Study area and site selection

This research was conducted in the southern coastal region of Denpasar City, Bali Province, Indonesia. Ecologically, this region is a dynamic estuary zone and tropical coastal wetland, influenced by tidal cycles and freshwater inputs from upstream areas. Over time, the southern coast of Denpasar has experienced massive anthropogenic land-cover changes, primarily driven by urbanization pressures and coastal development. These conditions make it a highly representative study site for observing the transition of coastal soil characteristics in response to human interventions (Dharmayasa et al., 2026; Widantara and Mutaqin, 2024).

Sampling was conducted using a purposive sampling technique to encompass five dominant land-cover typologies in the area. These five typologies were divided into two main categories: (1) natural to semi-natural ecosystems, comprising Mangrove Forests, Tidal Marshes, and Mudflats; and (2) anthropogenic or cultivated ecosystems, which include Paddy Fields and Aquaculture Ponds. Each land typology was represented by three replicate sampling points, yielding a total of 15 primary sample points. The study area and sampling locations are illustrated in Figure 2, while the geographic coordinates of the five sampling sites are presented in Table 1. At each representative site, three replicate sediment samples were collected within a short distance

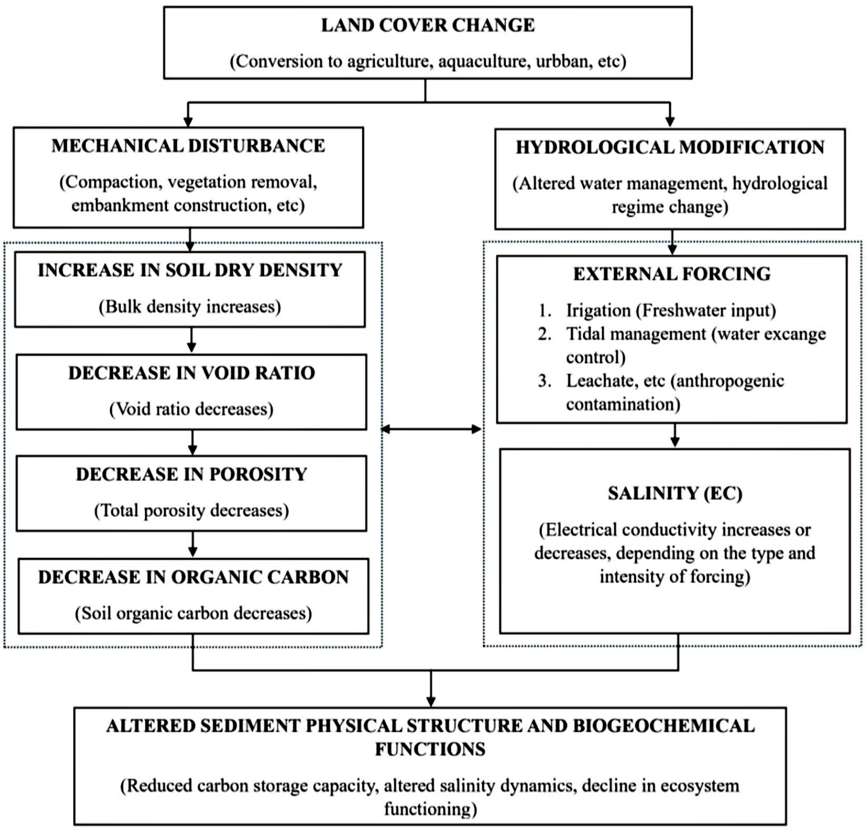

Figure 1. Conceptual framework illustrating the hypothesized relationships among land-cover change, sediment pore geometry, organic carbon retention, and salinity dynamics evaluated in this study

Figure 2. Map of study area, sampling locations and conditions

Table 1. Geographic coordinates of the representative sampling sites for each coastal land-use type

No	Land use type	Longitude (E)	Latitude (S)
1	Mangrove	115.2238894	-8.72050044
2	Mudflat	115.2137186	-8.72675431
3	Aquaculture pond	115.212833	-8.72380278
4	Marshland	115.2206343	-8.71705865
5	Paddy field	115.2442792	-8.69352606

(approximately 3–5 m) under similar geomorphological and land-use conditions. Because the replicate sampling site were closely spaced, only the representative GPS coordinate for each land-use type was recorded.

To ensure spatial representativeness and minimize bias caused by micro-local heterogeneity, each replicate was collected using a composite sampling technique. At each sample point, samples were taken from three random sub-points within a close radius. For biogeochemical and grain-size distribution analyses, disturbed soil samples from these three sub-points were thoroughly mixed (homogenized) at the upper soil profile depth (0–20 cm) before being transported to the laboratory. Meanwhile, undisturbed soil samples were collected using metal core rings at representative sub-points for the testing of physical and mechanical soil properties.

The entire field sampling campaign was conducted in June 2026, coinciding with the onset of the peak dry season in Bali Province. This period was intentionally selected (as a deliberate snapshot study) to evaluate the biophysical characteristics of the soil under extreme boundary conditions. During this period, the minimal freshwater input from precipitation triggers an evaporative concentration effect; thus, EC measurements can represent the maximum capacity of the soil matrix to retain salinity. Furthermore, dry season conditions minimize the leaching effect on soil organic matter and ensure that pore geometry indicators (void ratio and porosity) are measured under stable geomorphological structures, without distortion from seasonal pore water saturation fluctuations (Akça et al., 2020; Jha et al., 2023; Tang et al., 2023) (Figure 3).

Soil biogeochemical analysis

Biogeochemical parameters were evaluated to quantify carbon and salinity retention within the sediment matrix. SOC and EC were analyzed at the Soil Laboratory of the Agricultural Environmental Assessment and Development Center (BRMP Lingkungan), Ministry of Agriculture, Pati, Central Java, Indonesia, which is accredited by the Indonesian National Accreditation Committee (KAN) in accordance with ISO/IEC 17025:2017. All analyses were performed using validated standard laboratory methods in accordance with the laboratory's accredited quality assurance and quality control (QA/QC) system, including routine instrument calibration, method validation, and internal quality control procedures.

For the subsequent geotechnical analyses, the measured SOC content (%) was converted to SOM using the standard Van Bemmelen conversion factor (1.724), as follows (El Mouridi et al., 2023; Gerenfes et al., 2022):

$$\text{SOM (\%)} = \text{SOC (\%)} \times 1.724 \tag{1}$$

The calculated SOM values were subsequently used to estimate the theoretical specific gravity of the sediment solids (Gs) as part of the pore geometry reconstruction workflow. In addition, electrical conductivity (EC) was used as an indicator of sediment salinity and is reported in millisiemens per centimeter (mS/cm).

Physical and geotechnical index testing

Soil samples were analyzed to determine the physical index properties that form the basis for evaluating the geotechnical characteristics of the sediment. The principal laboratory instruments and apparatus used in the physical and geotechnical analyses are summarized in Table 2 to improve methodological transparency and reproducibility. All measuring instruments used in this study were periodically calibrated by an ISO/IEC 17025:2017-accredited calibration laboratory to ensure measurement accuracy and analytical reproducibility. Water content and bulk density were determined in duplicate for each sample, and the reported values represent the arithmetic mean of the two measurements to improve analytical repeatability. Grain-size distribution was determined by classifying the sediment into coarse fractions (sand) and fine fractions (silt and clay) based on the proportion of particles retained on and passing through the No. 200 sieve (0.075 mm aperture), following ASTM D6913 (ASTM, 2017). For the purposes of this study, sieve

Figure 3. Field data collection and laboratory documentation

Table 2. Laboratory instruments and apparatus used for physical and geotechnical index testing

No	Analysis	Instrument	Model
1	Water content	Drying oven	Memmert 854 Schwabach
2	Water content	Digital pecision Balance	ACIS AD-300i, readability 0.01 g
3	Water content	Aluminium container	Standard aluminum container
4	Bulk density	Digital pecision Balance	ACIS AD-300i, readability 0.01 g
5	Bulk density	Cylindrical sampling ring	Aluminum cylindrical sampling ring (volume: 15 cm^3)
6	Sieve analysis	Sieve shaker analysis	MBT AG-515
7	Sieve analysis	Standar sieve test	Sieve openings (4.75–0.075 mm)

analysis was considered sufficient to distinguish and characterize the coarse and fine particle fractions. All measuring instruments were periodically calibrated by an ISO/IEC 17025:2017-accredited calibration laboratory. Laboratory measurements were performed in accordance with standardized testing procedures to ensure measurement accuracy and analytical reproducibility.

For undisturbed samples, bulk density (ρ_b) was determined by direct measurement in accordance with ASTM D7263 (ASTM, 2021), while natural moisture content (w) was measured using the oven-drying method following ASTM D2216 (ASTM, 2019). Dry density (ρ_d) was then calculated from the fundamental mass–volume relationship between bulk density and natural moisture content, as expressed by Equation 2:

$$\rho_d = \frac{\rho_b}{1 + w} \quad (2)$$

where: ρ_d represents the dry density, ρ_d is the bulk density, and w denotes the natural moisture content expressed as a decimal.

This equation constitutes a fundamental mathematical relationship in soil mechanics that correlates bulk density, dry density, and moisture content, based on the principle of mass conservation.

Given the high variability of organic content among wetland types, the specific gravity (G_s) was estimated using a theoretical mixture equation based on mass and volume fractions (Adams, 1973; Rühlmann et al., 2006). This equation is expressed as:

$$G_s = \frac{100}{\frac{SOM}{G_{som}} + \frac{100 - SOM}{G_{sm}}} \quad (3)$$

where: G_s represents the specific gravity of the organic-mineral soil mixture, and SOM is the percentage of total organic matter.

The variables G_{som} and G_{sm} are the specific gravities of the pure organic component and the pure mineral component, respectively. To represent coastal geotechnical conditions accurately, G_{som} and G_{sm} were assigned standard geotechnical constants of 1.40 and 2.65. The 2.65 value represents the typical specific gravity of quartz-dominant mineral soils (Das, 2010), while the 1.40 value is a well-established constant for pure organic matter in geotechnical engineering (O'Kelly, 2017; Skempton and Petley, 1970).

Once the specific gravity (Gs) value was obtained, soil phase relationship parameters, including the void ratio (e) and porosity (n), were calculated based on fundamental phase relationships in soil mechanics. The calculation of the void ratio (e) is based on the relationship between specific gravity (G_s), dry density (ρ_d), and water density (ρ_w = 1 g/cm³), which is expressed as:

$$e = \left(\frac{G_s \times \rho_w}{\rho_d}\right) - 1 \quad (4)$$

where: e represents the void ratio, G_s is the specific gravity of the soil mixture, ρ_d is the dry density, and ρ_w is the water density, which is assumed to be 1 g/cm³.

Subsequently, the porosity value (n), which represents the percentage of void volume relative to the total volume of the soil matrix, was derived from the void ratio using the following equation:

$$n(\%) = \left(\frac{e}{1+e}\right) \times 100\% \quad (5)$$

where: n is the porosity (%), and e is the void ratio.

The sequence of calculations described above constitutes a physically consistent reconstruction procedure for estimating sediment pore geometry parameters from routinely measured laboratory data. Because the approach is based on fundamental mass–volume relationships and a theoretical mixture equation for estimating specific gravity, it can be readily reproduced and applied to coastal wetland sediments exhibiting variable organic matter contents. Consequently, this reproducible analytical workflow provides a physically consistent procedure for estimating pore geometry parameters from routinely measured laboratory data, facilitating integrated geotechnical and biogeochemical analyses across coastal wetland sediments with contrasting organic matter contents.

Statistical and spatial analysis

The compiled laboratory test data were processed using Microsoft Excel for data tabulation, calculation of derived parameters, and statistical analysis. Because the dataset comprised a relatively small sample size (N = 15) and the distribution of several variables was not assumed to satisfy normality, inferential analyses were conducted using non-parametric method (Cleophas and Zwinderman, 2016; Elliott and Hynan, 2011). Differences in physical index and biogeochemical parameters among the five independent land-cover types were evaluated using the Kruskal-Wallis test and post-hoc Dunn's Test using Minitab 19 application, a rank-based non-parametric alternative to one-way ANOVA for comparing more than two group (MacFarland and Yates, 2016; McKight and Najab, 2010; Ostertagová et al., 2014). Statistical significance was assessed at α = 0.05 to determine whether sediment properties differed among land-cover categories.

The relationships between soil pore geometry parameters and biogeochemical indicators were evaluated using Spearman's rank correlation coefficient (r_s) to determine the direction and strength of monotonic associations across land-cover types subjected to different levels of anthropogenic intervention (Bocianowski et al., 2024; Flanclin et al., 2024). To avoid statistical redundancy, significance testing was restricted to mathematically independent variable pairs.

Accordingly, porosity (n) was excluded because it is a direct function of void ratio (e), and SOM was not tested independently because it was derived from soil organic carbon (SOC). The correlation analysis therefore focused on three primary pairs: void ratio (e) – SOC, void ratio (e) – salinity (EC), and SOC – salinity (EC), using a significance threshold of α = 0.05.

Given the small group-wise sample size (n = 3), these inferential results should be interpreted strictly as exploratory baseline findings intended for hypothesis generation (Roberts et al., 2023). While small samples are not suitable for definitive population-level inferences or precise effect-size estimation (Kunselman, 2024; Leon et al., 2011), this initial exploratory framework combined with composite sampling is a necessary and highly valuable first step to justify and motivate substantially larger spatial sampling campaigns in future coastal wetland studies. In short, the correlation framework is methodologically appropriate, while the strength of inference is kept deliberately cautious, reflecting broader realities in ecological correlation analyses (Fox, 2025).

In addition to the statistical evaluation, the spatial distribution of sediment salinity was mapped to visualize the extent of potential anthropogenic influence. Spatial interpolation of EC values was conducted using the inverse distance weighting (IDW) method in ArcGIS 10.4 software. The IDW algorithm was specifically selected to effectively capture the localized diffusion pattern radiating from the highest EC concentration points, thereby providing a continuous and realistic spatial representation of salinity dispersion across the study area.

RESULT AND DISCUSSION

Physical index characteristics and reconstruction of soil pore geometry parameters

The physical characteristics of the soil in the southern coastal ecosystems of Denpasar exhibit variations that reflect the heterogeneity of land-cover conditions and local sedimentation processes. The results of the grain-size distribution analysis indicate that the majority of the samples are dominated by the sand fraction, with proportions ranging from 65.79% to 91.46%, while the fine-grained fraction (silt and clay) ranges from 8.54% to 34.21%. Based on this composition, the sedimentary material is generally classified as silty sand to clayey sand, indicating that the soil framework is primarily dominated by coarse grains with varying contributions from fine fractions.

Furthermore, the determination of pore geometry parameters requires a representative estimation of specific gravity (G_s) as a key phase relationship parameter in soil mechanics. Initial estimations utilizing the SOM values derived from the loss on ignition (LOI) method yielded G_s values lower than the theoretical range for organic-mineral soils. When these values were applied to calculate the void ratio (e) and porosity (n), the results were physically inconsistent with the characteristics of sand-dominated sediments.

To mitigate this inconsistency, the G_s estimation was subsequently reconstructed using the Theoretical Mixture Equation integrated with the Van Bemmelen chemical conversion factor (Equation 3). This approach yielded G_s values in the range of 2.51–2.63, which are more realistic and consistent with the observed coastal sediment characteristics. The reconstructed G_s values were then utilized to calculate the pore geometry parameters, specifically the void ratio (e) and porosity (n). A summary of the physical index characteristics and the reconstructed pore geometry parameters is presented in Table 3.

Based on Table 3, the reconstructed void ratio (e) and porosity (n) values fall within a physically realistic range for coastal wetland sediments. Among all sample groups, the aquaculture sites exhibited the lowest porosity values (37.97–45.47%), accompanied by the highest dry density (ρ_d) values (1.44–1.62 g/cm³), indicating a relatively denser sediment condition compared to the other land-cover groups. Conversely, the

Table 3. Physical index characteristics and reconstructed pore geometry parameters

Sample code	Total sand (%)	Fines (%)	SOC (g/kg)	W (%)	Estimated Gs	Dry density (g/cm³)	Void ratio (e)	Porosity (n) [%]	EC (mS/cm)
Mangrove 1	65.79	34.21	30.50	67.36	2.53	0.88	1.87	65.13	18.49
Mangrove 2	87.25	12.75	25.40	47.67	2.55	1.00	1.55	60.73	10.87
Mangrove 3	89.54	10.46	19.40	42.82	2.57	0.98	1.63	62.04	7.18
Mudflat 1	85.75	14.25	8.90	33.60	2.61	1.16	1.25	55.48	7.19
Mudflat 2	81.46	18.54	6.60	33.53	2.62	1.21	1.18	54.04	5.71
Mudflat 3	81.58	18.42	10.00	37.38	2.61	1.22	1.13	53.14	8.85
Marshland 1	84.96	15.04	27.30	54.39	2.54	1.06	1.41	58.49	0.60
Marshland 2	77.46	22.54	15.40	49.30	2.59	1.11	1.33	57.13	0.43
Marshland 3	81.67	18.33	35.30	46.77	2.51	1.07	1.34	57.28	0.48
Paddy field 1	77.81	22.19	15.30	41.46	2.59	1.20	1.16	53.67	0.11
Paddy field 2	82.50	17.50	20.90	53.53	2.57	1.03	1.51	60.09	0.13
Paddy field 3	82.75	17.25	14.50	29.75	2.59	1.54	0.68	40.45	0.18
Aquaculture pond 1	88.00	12.00	9.30	31.05	2.61	1.51	0.73	42.08	4.60
Aquaculture pond 2	91.46	8.54	8.40	28.98	2.62	1.62	0.61	37.97	4.26
Aquaculture pond 3	91.37	8.63	3.80	25.77	2.64	1.44	0.83	45.47	3.91

mangrove, mudflat, and marshland groups generally possessed higher porosity values, reflecting a looser sediment structure.

In general, an increase in dry density (ρ_d) was followed by a decrease in void ratio (e) and porosity (n), consistent with the principles of phase relationships in soil mechanics. Samples with a higher dry density (ρ_d) tended to have a smaller void volume, thereby resulting in lower void ratio and porosity values (Hou et al., 2025; Okovido and Obroku, 2021; Wei et al., 2024). The consistency of these relationships demonstrates that the reconstructed specific gravity (G_s), dry density (ρ_d), void ratio (e), and porosity (n) values can logically and consistently represent the physical conditions of the sediment. Consequently, these values can be reliably utilized as a basis for analyzing the interplay between physical characteristics, biogeochemical properties, and land-cover changes in the subsequent sections (Benjamin et al., 2026; Kurek et al., 2024).

Beyond improving the internal consistency of the calculated physical parameters, the analytical workflow adopted in this study provides a practical framework for integrating sediment physical and biogeochemical properties. Because the workflow is based entirely on established soil mechanics equations, its primary contribution lies in facilitating reproducible interdisciplinary analyses rather than introducing a new computational method.

The value of this integrated analytical workflow is reflected in the interpretation of the study results. Rather than simply confirming previously reported relationships between anthropogenic land-use change and sediment degradation, the present study suggests that the reconstructed pore geometry framework provides a practical means of integrating routinely measured geotechnical and biogeochemical properties for assessing sediment condition in coastal wetlands. The contrasting relationships observed between pore geometry, soil organic carbon, and salinity indicate that sediment structural degradation and salinity dynamics are governed by different controlling mechanisms. Whereas soil organic carbon was closely associated with pore architecture, salinity variability appeared to be influenced by factors beyond sediment pore geometry, including external environmental and anthropogenic conditions. This distinction provides a more comprehensive framework for interpreting coastal wetland degradation by linking sediment structural integrity with ecosystem functioning, rather than evaluating physical or biogeochemical properties independently.

Relationship between pore geometry and biogeochemical indicators

Spearman's rank correlation analysis (r_s) was utilized to evaluate the strength and direction of the relationships between pore geometry parameters and soil biogeochemical indicators. The results of the statistical significance testing (p-value < 0.05) are presented in Table 3.

The test results in Table 4 reveal a strong and statistically significant positive correlation between pore geometry parameters (void ratio and porosity) and SOC content (r_s = 0.757; p = 0.001). This finding indicates a strong association between the development of pore structure and the accumulation of organic carbon within the sedimentary matrix (Bhattacharyya et al., 2021; Fukumasu et al., 2022; Z. Zhao et al., 2024). Although correlation analysis cannot be used to infer causal relationships, these results suggest that both parameters develop interdependently in response to the same environmental conditions and sedimentary processes.

Conceptually, this relationship can be explained through the reciprocal interaction between physical and biogeochemical soil processes (Bucka et al., 2019). On the one hand, the accumulation of organic matter originating from vegetation litter is presumed to contribute to maintaining the soil aggregate structure and the pore spaces between mineral grains, thereby reducing the tendency for sediment compaction (Fukumasu et al., 2022; Rabbi et al., 2024). On the other hand, a soil matrix with a higher void ratio (e) and porosity provides greater accommodation space for the accumulation and retention of organic material. This condition allows organic matter to be more readily stored within the sediment matrix while simultaneously retarding the loss of organic material driven by hydrological transport processes. Therefore, high SOC content in coastal sediments tends to associate with a more developed pore geometry structure and greater pore space capacity (Bucka et al., 2019; Rabbi et al., 2024).

Table 4 presents the Spearman correlation coefficient matrix for all analyzed parameters as a general overview of the inter-variable relationships. As explained in Subsection "Physical Index Characteristics and Reconstruction of Soil Pore Geometry Parameters", several variable pairs possess mathematically deterministic relationships; hence, subsequent statistical significance testing was solely performed on mathematically independent variable pairs.

Based on the significance test results in Table 5, the positive relationship between void ratio (e) and SOC is proven to be statistically significant (r_s = 0.757; p = 0.001). Conversely, the relationships between void ratio and salinity (EC), as well as between SOC and salinity, do not demonstrate statistical significance ($p > 0.05$). This finding indicates that variations in sediment pore geometry are more closely associated with organic matter content than with salinity levels at the study site.

Although several statistically significant Spearman correlations were identified, these relationships should be interpreted cautiously because the analysis was based on a relatively small number of observations (n = 15). Consequently, the reported correlation coefficients are intended to provide exploratory evidence of associations among sediment pore geometry and biogeochemical properties rather than definitive statistical relationships. Future investigations involving larger sample sizes and broader spatial coverage are required to verify the robustness and general applicability of the observed correlation

Salinity variations in coastal sediments and anthropogenic influence

The variation in EC values across the sample groups exhibits a highly broad range, from 0.11 mS/cm in the paddy field group to 18.49 mS/cm in the mangrove group. Based on the Spearman correlation test results (Table 4), the EC values do not demonstrate a statistically significant relationship with pore geometry parameters (r_s = 0.296; p = 0.284) or SOC content (r_s = -0.036; p = 0.899). These results indicate that the salinity variations at the study site are not directly associated with the physical characteristics or the organic matter content of the sediment.

Table 4. Spearman's rank correlation matrix among soil pore geometry and biogeochemical parameters

Variables	Void ratio (e)	Porosity (n)	SOC	SOM	Salinity (EC)
Void ratio (e)	1.000	1.000	0.757	0.757	0.296
Porosity (n)	1.000	1.000	0.757	0.757	0.296
SOC	0.757	0.757	1.000	1.000	-0.036
SOM	0.757	0.757	1.000	1.000	-0.036
Salinity (EC)	0.296	0.296	-0.036	-0.036	1.000

Table 5. Significance test results for Spearman's rank correlation on key variable pairs

Variable pair	Correlation coefficient (r_s)	p-value (2-tailed)	Significance
Void ratio (e) and SOC / SOM	0.757	0.001	Significant
Void ratio (e) and salinity (EC)	0.296	0.284	Not Significant
SOC / SOM and salinity (EC)	-0.036	0.899	Not Significant

The spatial variation of EC values, as illustrated in Figure 4, reveals that the Mangrove (3) group possesses significantly higher EC values compared to the other locations. Visually, the spatial interpolation in Figure 4 displays a clear diffusion pattern where the highest EC values (indicated by the red and orange zones of 16–20 mS/cm) are concentrated directly adjacent to the Suwung Landfill, before gradually dissipating toward the surrounding waters of Benoa Bay and Serangan Island. This spatial pattern visually demonstrates that changes in salinity do not align with variations in pore geometry parameters or SOC content. In line with the Spearman correlation test results (Table 4), this condition suggests that the salinity distribution at the study site is likely more influenced by external factors rather than by the intrinsic properties of the sediment.

The finding of no significant relationship between salinity and pore geometry parameters provides an indication that the initial hypothesis of this study is not fully supported. It was initially hypothesized that land-use conversion would modify sediment pore geometry, potentially influencing water movement within the sediment

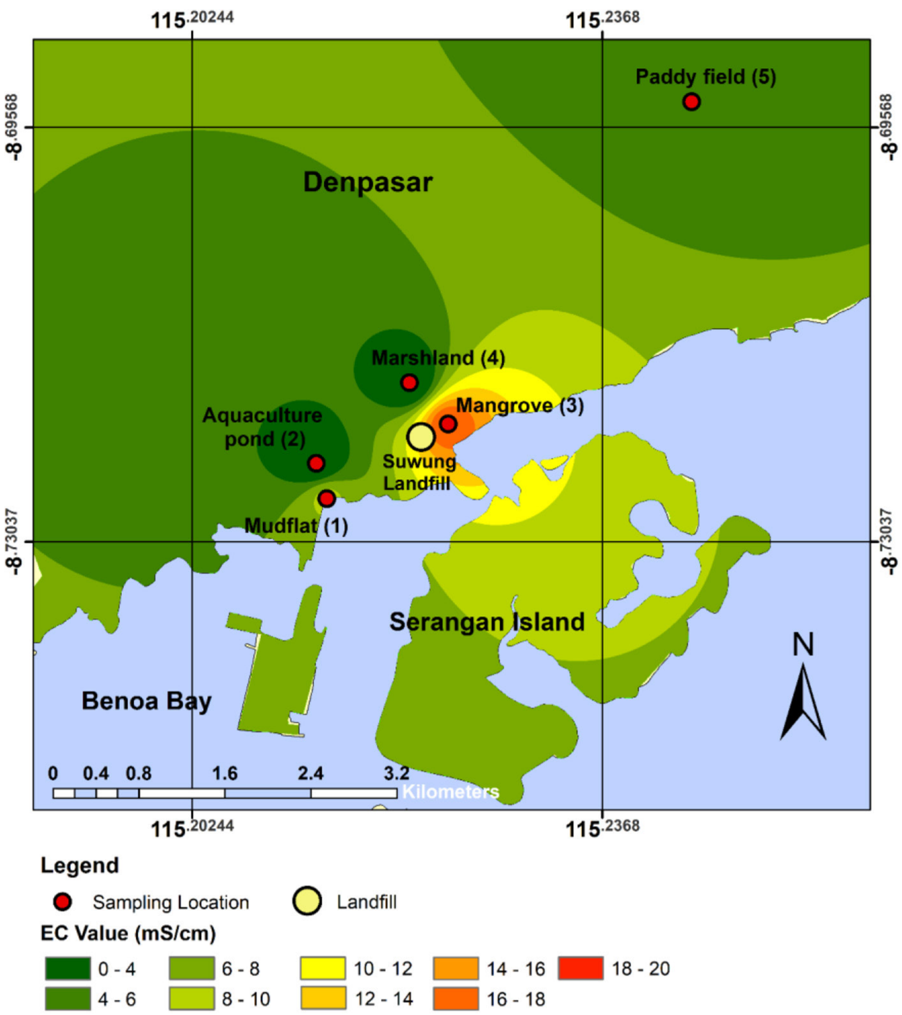

Figure 4. Spatial distribution of electrical conductivity (EC) across the study area

and consequently affecting salinity conditions. However, the research findings reveal that this mechanism is not markedly evident at the study site. These observations suggest that factors other than sediment pore geometry may contribute more substantially to EC variability across the investigated sites (Feng and Chen, 2023; Marchand et al., 2004; Zhu et al., 2024).

One plausible explanation is the influence of water management modifications driven by anthropogenic activities (Han and Currell, 2018). In paddy fields, continuous freshwater irrigation processes potentially induce salt leaching, thereby resulting in relatively low EC values (Wang et al., 2017; Y. Zhang et al., 2021). Conversely, in aquaculture pond areas, tidal management for cultivation activities is presumed to influence sediment salinity dynamics (Yang et al., 2025). On the other hand, the exceptionally high EC values observed in the mangrove group, which is located adjacent to the Suwung Landfill area, may reflect the influence of external environmental or anthropogenic factors beyond sediment pore geometry. (Herbert et al., 2015; Kaushal et al., 2021). However, because no hydrochemical tracers or diagnostic chemical markers were analyzed, the specific sources of dissolved ions cannot be identified from the present dataset. Accordingly, no attribution to a specific contamination source can be made based on the present dataset. Future investigations incorporating hydrochemical characterization and chemical tracer analyses are required to identify the origin of the dissolved ions responsible for the observed EC variability.

Overall, the results indicate that salinity variability cannot be explained solely by sediment pore geometry or soil organic carbon. Instead, the findings suggest that multiple environmental factors beyond the measured sediment properties may contribute to EC variability across the investigated sites. Because the origin of dissolved ions was not investigated directly, no specific contamination source can be identified from the present dataset.

Impacts of anthropogenic intervention and land-use conversion on soil characteristics

To evaluate the influence of anthropogenic intervention on the physical and biogeochemical characteristics of coastal sediments, the soil samples were classified into two primary categories: natural/semi-natural land (mangrove, mudflat, marshland) and anthropogenically intervened land (paddy field, aquaculture). The Kruskal-Wallis statistical test results confirmed that these variations in land cover yielded statistically significant differences ($p < 0.05$) across all key parameters, including soil porosity, SOC retention, and salinity accumulation, as summarized in Table 6.

The Kruskal-Wallis test results demonstrate that land-cover types are significantly associated with variations in porosity, SOC content, and salinity (Figure 5). These findings indicate that land-cover change is a crucial factor influencing the physical and biogeochemical characteristics of coastal sediments (J. Li et al., 2024; Sasmito et al., 2020). The underlying mechanisms driving these differences are subsequently discussed based on alterations in pore geometry, organic carbon dynamics, and salinity conditions within each land-cover type (Dale et al., 2019; R. Zhang et al., 2025).

Pore geometry degradation due to mechanical compaction

The most striking differences are observed in the physical index and pore geometry parameters. The natural land group (mangrove, mudflat, marshland) consistently exhibited higher void ratio (e) values (ranging from 1.13 to 1.86) and high porosity (n) (53–65%). This loose soil structure is maintained by the presence of natural vegetation root systems and the accumulation of organic litter, which prevents excessive compaction of the sediment matrix. Conversely, in anthropogenically disturbed lands, particularly in aquaculture ponds, there was a drastic reduction in porosity to merely 37–45%, accompanied by an increase in dry density (ρ_d) reaching 1.43–1.62 g/cm³.

Table 6. Summary of Kruskal-Wallis test results across land-cover types

Parameter	H-statistic	df	p-value*	Conclusion
Void ratio (e)	10.93	4	< 0.05	Significant
SOC	11.43	4	< 0.05	Significant
Salinity (EC)	13.04	4	< 0.05	Significant

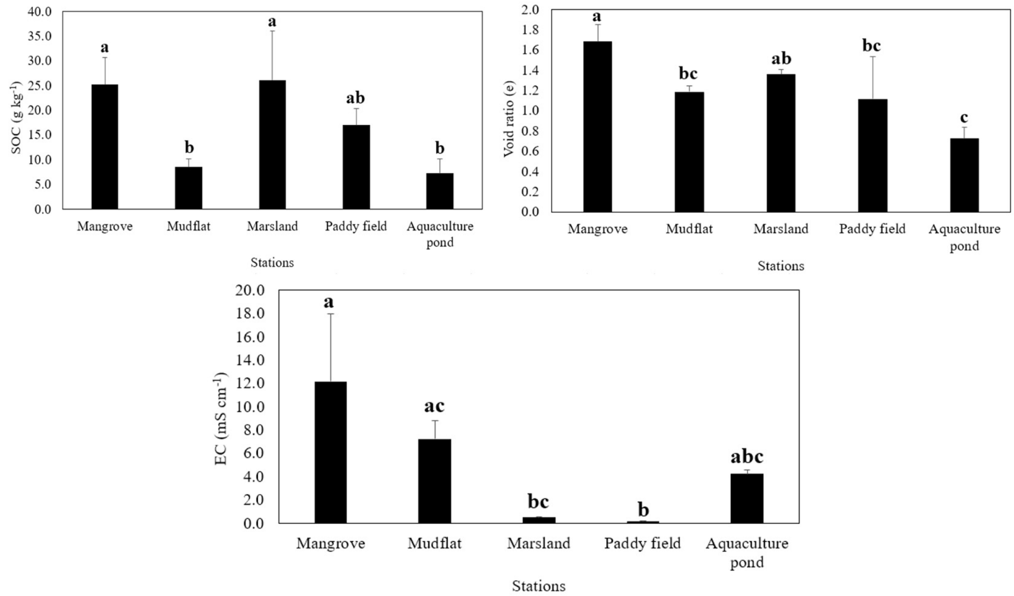

Figure 5. Average and Kruskal-Wallis to Dun's test result on key parameters

This extreme reduction in pore space is presumed to be associated with compaction activities during the construction of aquaculture ponds, as a direct consequence of human mechanical intervention (Van Wesenbeeck et al., 2015). The development of cultivation ponds necessitates intentional soil compaction to construct water-impermeable and geotechnically stable embankments (Vo Ai Mi, 2023). Consequently, this diminishes the void volume, eliminating the natural function of the soil as a sponge for water and carbon storage (Hongwiset et al., 2022).

From a soil mechanics perspective, this extreme compaction provides a short-term geotechnical advantage by increasing the shallow bearing capacity required to support anthropogenic infrastructure, such as pond embankments (Vo Ai Mi, 2023). However, these observed differences in sediment structure may have implications for long-term geotechnical behaviour, as suggested in previous studies. The observed reduction in pore volume is consistent with sediment conditions that have been associated in previous studies with lower permeability and altered consolidation behaviour, although these processes were not directly evaluated in the present study (Galloway et al., 2016). When coupled with the observed reduction in SOC, these sediment characteristics are consistent with conditions that have been associated with increased susceptibility to differential settlement and localized land subsidence in previous studies, although these responses were not directly measured in the present investigation.

The structural degradation observed in this study carries implications that extend beyond localized physical modifications. Progressive sediment compaction and porosity loss have been widely reported as factors associated with increased land subsidence in coastal environments. The sediment characteristics observed in the present study are consistent with these reported relationships; however, land subsidence was not directly measured (Y. Chen et al., 2018; Dharmayasa et al., 2026). The observed reduction in pore space may influence the mechanical behaviour of sediments, although parameters such as bearing capacity and consolidation rate were beyond the scope of the present study (G. Chen et al., 2023). Under conditions of sea-level rise, similar sediment characteristics have been reported to coincide with greater vulnerability of coastal environments; however, these broader geomorphological implications were not evaluated in the present study (Van Wesenbeeck et al., 2015). These findings support the importance of preserving sediment pore geometry as a useful indicator of sediment structural condition that may contribute to broader assessments of coastal resilience when integrated with complementary hydrological and geomorphological information (Van Bijsterveldt et al., 2020). It should be emphasized that the present study did not directly measure permeability, consolidation behaviour, settlement, or land subsidence. Therefore, the above interpretations are presented as plausible implications supported by established soil mechanics theory and previous studies rather than as direct outcomes demonstrated by the present dataset.

Soil organic carbon depletion in disturbed lands

From a biogeochemical perspective, anthropogenic interventions trigger severe depletion of soil organic content. Natural areas such as marshlands and mangroves are capable of retaining SOC at relatively high ranges (15.4 to 35.3 g/kg). The presence of mangrove vegetation, which continuously supplies organic matter (leaf litter), supports a healthy carbon cycle (X. Chen et al., 2021).

On the other hand, aquaculture land recorded the lowest SOC in this study (only 3.8 to 9.3 g/kg). The clearing of pond areas typically involves topsoil stripping, which removes organic-rich layers, and the total clear-cutting of vegetative cover (Fu et al., 2025; Xia et al., 2022). Although paddy fields are also disturbed lands, the reduction in SOC was not as extreme as in aquaculture (ranging from 14.5 to 20.9 g/kg). This is logical considering that rice cultivation still leaves behind rice stubble and frequently receives additional inputs of organic fertilizers, which help maintain a portion of the carbon fraction within the soil (D. Zhao et al., 2020).

The decline in SOC content in aquaculture areas also holds implications for the carbon storage function of coastal wetland ecosystems (Hao et al., 2024). Mangroves and marshlands are recognized as critical components of blue carbon ecosystems due to their capacity to accumulate organic carbon in sediments over long periods (Piñeiro-Juncal et al., 2025). Therefore, the reduced SOC content observed in converted lands indicates a potential decrease in carbon storage capacity compared to natural conditions (Fu et al., 2025). Although this study did not directly evaluate carbon stocks or fluxes, these findings align with various studies reporting that the conversion of coastal wetlands can diminish carbon storage functions and associated ecosystem services.

Hydrodynamic and salinity modification

Land-use conversion also artificially alters the salinity regime (Glamore et al., 2021). In the anthropogenic land group, EC values reflect the designated purpose of the land. Aquaculture ponds utilized for brackish water cultivation exhibit salinity maintained at moderate levels (3.91–4.60 mS/cm) through tidal sluice gate management. Conversely, paddy fields possess the lowest EC values, approaching zero (0.11–0.18 mS/cm). These figures indicate the occurrence of massive salt leaching processes resulting from hydrological modifications, specifically continuous freshwater irrigation that inundates the rice fields (White and Kaplan, 2017).

Interestingly, although the mangrove group is classified as natural land (functioning as a buffer zone), this location actually recorded exceptionally high salinity (EC up to 18.49 mS/cm). This indicates that preserving land cover alone is insufficient if, spatially, the natural land is situated adjacent to destructive anthropogenic pollution sources (such as exposure to leachate from the Suwung Landfill) (Chi et al., 2019; Islam et al., 2023). This condition demonstrates that spatial proximity to anthropogenic pollutant sources can potentially affect sediment quality (Herbert et al., 2015).

Overall, the findings were generally consistent with the proposed conceptual hypothesis. Anthropogenic land-cover conversion was associated with measurable modifications of sediment pore geometry and organic carbon retention (Newton et al., 2020). However, the expected relationship between pore geometry and salinity was not evident, indicating that salinity dynamics in the studied coastal wetlands are more strongly influenced by external hydrological and anthropogenic processes than by the intrinsic physical characteristics of the sediment matrix (Xin et al., 2022).

Comparison of reconstructed specific gravity with independent laboratory measurements

To evaluate the reliability of the reconstructed specific gravity (G_s), the estimated values were compared with independently measured G_s values obtained from representative coastal sediments in southern Bali (Table 7). Although these laboratory measurements were collected from different sampling sites and therefore do not constitute a direct sample-to-sample validation, they provide an appropriate regional reference for assessing whether the reconstructed G_s values are physically realistic and consistent with the range expected for coastal wetland sediments.

As shown in Table 7, the reconstructed G_s values ranged from 2.51 to 2.64, whereas the independently measured laboratory values ranged from 2.07 to 2.73, reflecting the natural variability in sediment composition among different coastal environments in southern Bali. The lower laboratory G_s values are associated with sediments containing higher proportions of organic material, whereas the higher values represent more mineral-dominated sandy sediments. The reconstructed G_s values are concentrated within the mineral-dominated portion of this regional range, which is consistent with the relatively low to moderate organic matter contents observed in most samples of the present study.

Because the independent laboratory data were obtained from different sampling locations, the comparison should be interpreted as an assessment of the physical plausibility of the reconstructed G_s values rather than as a direct sample-to-sample validation. Nevertheless, the comparison demonstrates that the reconstructed G_s values are consistent with the broader range of independently measured G_s reported for representative coastal sediments in southern Bali, supporting their use within the proposed analytical workflow. Since void ratio (e) and porosity (n) were not independently measured but were derived from the reconstructed G_s and experimentally determined dry bulk density (ρ_d) using established soil phase relationships, the reliability of these derived parameters depends primarily on the reliability of the reconstructed Gs estimates. Therefore, the independent comparison of Gs also provides indirect support for the subsequent calculations of e and n. However, because neither Gs nor the derived pore geometry parameters were verified using the same sediment samples, this comparison should be regarded as an independent regional assessment rather than definitive validation. Future studies incorporating direct ASTM D854 measurements together with independent determinations of pore geometry on the same sediment samples are recommended to provide a more rigorous verification of the proposed reconstruction approach.

Study limitations and future research

Although the present study provides consistent evidence of the relationships between sediment pore geometry and biogeochemical characteristics across five contrasting coastal land-use types, several limitations should be acknowledged when interpreting the broader applicability of the findings.

First, the relatively small sample size (n = 3 per land-use type; total n = 15) reflects the logistical constraints associated with detailed laboratory characterization of coastal wetland sediments. Consequently, the results should be interpreted within the environmental setting of the investigated sites and should not be generalized directly to other coastal wetland systems without further validation. This limitation also affects the statistical power of the correlation analysis. Although Spearman's rank correlation is appropriate for small, non-parametric datasets, the resulting relationships should be regarded as exploratory and require confirmation using larger datasets encompassing a broader range of coastal wetland environments.

Second, the reconstructed pore geometry parameters were derived from established soil mechanics equations using routinely measured laboratory variables rather than direct measurements obtained from advanced imaging techniques such as X-ray computed tomography (CT) or scanning electron microscopy (SEM). Accordingly, the present workflow is intended to provide a practical and reproducible analytical framework for integrated geotechnical–biogeochemical assessment rather than a direct characterization of sediment microstructure.

Despite these limitations, the consistency of the observed relationships across the five

Table 7. Comparison of reconstructed specific gravity (Gs) values with independent laboratory measurements from representative coastal sediments in southern Bali

Land-use category	Reconstructed G_s	Independent laboratory G_s (southern Bali)
Mangrove	2.53–2.57	2.07–2.46
Marshland	2.51–2.59	–
Mudflat	2.61–2.62	2.73 (sand flat)
Paddy field	2.57–2.59	2.29–2.38 (agricultural soils)
Aquaculture pond	2.61–2.64	2.14 (aquaculture sediment)

contrasting land-use types supports the usefulness of the integrated analytical workflow for evaluating the interactions between sediment pore geometry, soil organic carbon retention, and sediment salinity. Future studies should include larger sample sizes, broader geographic coverage, seasonal observations, and independent validation datasets to assess the robustness and transferability of the proposed analytical framework across different coastal wetland environments. In addition, integrating direct pore-scale imaging techniques with the present analytical workflow would provide further insight into the mechanisms linking sediment structure and ecosystem functioning under anthropogenic land-use change.

CONCLUSIONS

This study demonstrates that the primary contribution does not lie in introducing a new geotechnical calculation method, but in integrating reconstructed pore geometry parameters with biogeochemical indicators within a reproducible analytical workflow for evaluating coastal wetland sediments. By combining established soil mechanics principles with biogeochemical assessment, the proposed framework enables physically consistent interpretation of sediment structural condition across contrasting coastal land-use types.

The results showed that reconstructed pore geometry parameters were strongly associated with soil organic carbon, suggesting that sediment pore architecture is closely linked to carbon retention across the investigated coastal wetland sites. In contrast, the absence of a significant relationship between pore geometry and electrical conductivity suggests that salinity variability may be influenced more strongly by external hydrological conditions and anthropogenic activities than by sediment structural characteristics. These contrasting responses suggest that different ecosystem functions may respond to different controlling factors, providing a more comprehensive interpretation of coastal wetland degradation than evaluating physical or biogeochemical properties independently.

Overall, the interdisciplinary integration of geotechnical and biogeochemical analyses provides a practical framework for assessing sediment structural integrity and ecosystem functioning using routinely measured laboratory data. Although the analytical workflow relies entirely on established soil mechanics equations, its reproducible implementation offers a useful approach for integrated environmental assessment and supports future investigations of anthropogenic impacts on tropical coastal wetlands.

Acknowledgements

The authors sincerely thank Universitas Pendidikan Nasional (UNDIKNAS) for providing access to laboratory facilities that made this research possible. The authors declare that they have no competing interests or conflicts of interest regarding the publication of this manuscript.

REFERENCES

1. Adams, W. A. (1973). The effect of organic matter on the bulk and true densities of some uncultivated podzolic soils. *Journal of Soil Science*, *24*(1), 10–17. https://doi.org/10.1111/j.1365-2389.1973.tb00737.x
2. Akça, E., Aydin, M., Kapur, S., Kume, T., Nagano, T., Watanabe, T., Çilek, A., Zorlu, K. (2020). Long-term monitoring of soil salinity in a semi-arid environment of Turkey. *CATENA*, *193*, 104614. https://doi.org/10.1016/j.catena.2020.104614
3. Alharbi, H. S. (2025). Geotechnical controls on land degradation in drylands: Indicators and mitigation for infrastructure and renewable energy. *Sustainability*, *18*(1), 242. https://doi.org/10.3390/su18010242
4. ASTM. (2019). *Standard Test Methods for Laboratory Determination of Water (Moisture) Content of Soil and Rock by Mass (ASTM D2216-19)*. ASTM International.
5. ASTM. (2021). *Standard Test Methods for Laboratory Determination of Density (Unit Weight) of Soil Specimens (ASTM D7263-21)*. ASTM International.
6. Benjamin, A., Bénédicte, D., Chaumillon, E., Rumpel, C., Dignac, M.-F., Felbacq, A., Schmidt, S., Destampes, M., Arnaud, M., Metzger, E., Lacoue-Labarthe, T., Dupuy, C. (2026). Organic carbon composition and preservation in macrotidal coastal wetland sediment: Insights from biomarkers and isotopic signatures. *Science of The Total Environment*, *1020*, 181542. https://doi.org/10.1016/j.scitotenv.2026.181542
7. Bhattacharyya, R., Rabbi, S. M. F., Zhang, Y., Young, I. M., Jones, A. R., Dennis, P. G., Menzies, N. W., Kopittke, P. M., Dalal, R. C. (2021). Soil organic carbon is significantly associated with the pore geometry, microbial diversity and enzyme activity of the macro-aggregates under different land uses. *Science of The Total Environment*, *778*, 146286. https://

doi.org/10.1016/j.scitotenv.2021.146286

8. Bocianowski, J., Wrońska-Pilarek, D., Krysztofiak-Kaniewska, A., Matusiak, K., Wiatrowska, B. (2024). Comparison of Pearson's and Spearman's correlation coefficients for selected traits of *Pinus sylvestris* L. *Biometrical Letters*, *61*(2), 115–135. https://doi.org/10.2478/bile-2024-0008
9. Brown, C. J., Adame, M. F., Buelow, C. A., Frassl, M. A., Lee, S. Y., Mackey, B., McClure, E. C., Pearson, R. M., Rajkaran, A., Rayner, T. S., Sievers, M., Saint Ange, C. A., Sousa, A. I., Tulloch, V. J. D., Turschwell, M. P., Connolly, R. M. (2021). Opportunities for improving recognition of coastal wetlands in global ecosystem assessment frameworks. *Ecological Indicators*, *126*, 107694. https://doi.org/10.1016/j.ecolind.2021.107694
10. Bucka, F. B., Kölbl, A., Uteau, D., Peth, S., Kögel-Knabner, I. (2019). Organic matter input determines structure development and aggregate formation in artificial soils. *Geoderma*, *354*, 113881. https://doi.org/10.1016/j.geoderma.2019.113881
11. Chen, G., Hong, W., Gu, X., Krauss, K. W., Zhao, K., Fu, H., Chen, L., Wang, M., Wang, W. (2023). Coupling near-surface geomorphology with mangrove community diversity at the estuarine scale: A case study at Dongzhaigang Bay, China. *Sedimentology*, *70*(1), 31–47. https://doi.org/10.1111/sed.13030
12. Chen, X., Hu, Y., Xia, Y., Zheng, S., Ma, C., Rui, Y., He, H., Huang, D., Zhang, Z., Ge, T., Wu, J., Guggenberger, G., Kuzyakov, Y., Su, Y. (2021). Contrasting pathways of carbon sequestration in paddy and upland soils. *Global Change Biology*, *27*(11), 2478–2490. https://doi.org/10.1111/gcb.15595
13. Chen, Y., Li, Y., Thompson, C., Wang, X., Cai, T., Chang, Y. (2018). Differential sediment trapping abilities of mangrove and saltmarsh vegetation in a subtropical estuary. *Geomorphology*, *318*, 270–282. https://doi.org/10.1016/j.geomorph.2018.06.018
14. Chi, Y., Sun, J., Liu, W., Wang, J., Zhao, M. (2019). Mapping coastal wetland soil salinity in different seasons using an improved comprehensive land surface factor system. *Ecological Indicators*, *107*, 105517. https://doi.org/10.1016/j.ecolind.2019.105517
15. Christiawan, P. I., Nguyen, T. P. L. (2024). Re-framing the interlinked between demographic transition and land-use change in developing countries periurbanization. *Indonesian Journal of Geography*, *56*(3). https://doi.org/10.22146/ijg.89118
16. Cleophas, T. J., Zwinderman, A. H. (2016). Non-parametric Tests for Three or More Samples (Friedman and Kruskal-Wallis). In T. J. Cleophas & A. H. Zwinderman, *Clinical Data Analysis on a Pocket Calculator* (pp. 193–197). Springer International Publishing. https://doi.org/10.1007/978-3-319-27104-0_34
17. Dale, J., Cundy, A. B., Spencer, K. L., Carr, S. J., Croudace, I. W., Burgess, H. M., Nash, D. J. (2019). Sediment structure and physicochemical changes following tidal inundation at a large open coast managed realignment site. *Science of The Total Environment*, *660*, 1419–1432. https://doi.org/10.1016/j.scitotenv.2018.12.323
18. Das, B. M. (2010). *Principles of Geotechnical Engineering* (7th ed.). Cengage Learning.
19. Dharmayasa, I. G. N. P., Sugiana, I. P., Meidudga, R. E. (2026). High subsidence vulnerability in Denpasar's coastal wetlands: Geotechnical characterisation of soft soils and implications for sustainable zoning. *Ecological Engineering & Environmental Technology*, *27*(1), 265–276. https://doi.org/10.12912/27197050/215576
20. El Mouridi, Z., Ziri, R., Douaik, A., Bennani, S., Lembaid, I., Bouharou, L., Brhadda, N., Moussadek, R. (2023). Comparison between Walkley-Black and loss on ignition methods for organic matter estimation in different Moroccan soils. *Ecological Engineering & Environmental Technology*, *24*(4), 253–259. https://doi.org/10.12912/27197050/163121
21. Elliott, A. C., Hynan, L. S. (2011). A SAS® macro implementation of a multiple comparison post hoc test for a Kruskal–Wallis analysis. *Computer Methods and Programs in Biomedicine*, *102*(1), 75–80. https://doi.org/10.1016/j.cmpb.2010.11.002
22. Feng, X., Chen, J. (2023). Impacts of environmental factors and freshwater discharges from multiple river outlets on estuarine salinity variation in rainy season: A case study of the Pearl River Estuary in China. *Journal of Hydrology*, *623*, 129784. https://doi.org/10.1016/j.jhydrol.2023.129784
23. Flanclin, N. N. B. V., Victor, K. J., Lucas, K., Tambou, T. B. Ii. H. D. (2024). Predicting soil parameters in Maroua 1st, Cameroon, using correlations of geophysical and geotechnical data. *Heliyon*, *10*(8), e29589. https://doi.org/10.1016/j.heliyon.2024.e29589
24. Fox, J. W. (2025). The sample size of the typical ecological correlation coefficient is small and slowly declining. *Oikos*, *2025*(12), e11430. https://doi.org/10.1002/oik.11430
25. Fu, C., Klein, S. G., Breavington, J., Lim, K. K., Steckbauer, A., Duarte, C. M. (2025). Nonuniform organic carbon stock loss in soils across disturbed blue carbon ecosystems. *Nature Communications*, *16*(1), 4370. https://doi.org/10.1038/s41467-025-59752-9
26. Fukumasu, J., Jarvis, N., Koestel, J., Kätterer, T., Larsbo, M. (2022). Relations between soil organic carbon content and the pore size distribution for an arable topsoil with large variations in soil properties. *European Journal of Soil Science*, *73*(1), e13212. https://doi.org/10.1111/ejss.13212
27. Galloway, D. L., Erkens, G., Kuniansky, E. L., Rowland, J. C. (2016). Preface: Land subsidence processes. *Hydrogeology Journal*, *24*(3), 547–550.

https://doi.org/10.1007/s10040-016-1386-y

28. Gerenfes, D., Giorgis, A. G., Negasa, G. (2022). Comparison of organic matter determination methods in soil by loss on ignition and potassium dichromate method. *International Journal of Horticulture and Food Science*, *4*(1), 49–53. https://doi.org/10.33545/26631067.2022.v4.i1a.85
29. Glamore, W., Rayner, D., Ruprecht, J., Sadat-Noori, M., Khojasteh, D. (2021). Eco-hydrology as a driver for tidal restoration: Observations from a Ramsar wetland in eastern Australia. *PLOS ONE*, *16*(8), e0254701. https://doi.org/10.1371/journal.pone.0254701
30. Han, D., Currell, M. J. (2018). Delineating multiple salinization processes in a coastal plain aquifer, northern China: Hydrochemical and isotopic evidence. *Hydrology and Earth System Sciences*, *22*(6), 3473–3491. https://doi.org/10.5194/hess-22-3473-2018
31. Hao, Q., Song, Z., Zhang, X., He, D., Guo, L., Van Zwieten, L., Yu, C., Wang, Y., Wang, W., Fang, Y., Fang, Y., Liu, C.-Q., Wang, H. (2024). Organic blue carbon sequestration in vegetated coastal wetlands: Processes and influencing factors. *Earth-Science Reviews*, *255*, 104853. https://doi.org/10.1016/j.earscirev.2024.104853
32. He, Q., Li, Z., Elphick, C. S., Sun, Y., Sutherland, W. J., Taylor, N. G., Wasson, K. (2025). Making restoration effective for dynamic coastal wetlands. *Global Change Biology*, *31*(9), e70455. https://doi.org/10.1111/gcb.70455
33. Herbert, E. R., Boon, P., Burgin, A. J., Neubauer, S. C., Franklin, R. B., Ardón, M., Hopfensperger, K. N., Lamers, L. P. M., Gell, P. (2015). A global perspective on wetland salinization: Ecological consequences of a growing threat to freshwater wetlands. *Ecosphere*, *6*(10), 1–43. https://doi.org/10.1890/ES14-00534.1
34. Hongwiset, S., Rodtassana, C., Poungparn, S., Umnouysin, S., Suchewaboripont, V. (2022). Synergetic roles of mangrove vegetation on sediment accretion in coastal mangrove plantations in central Thailand. *Forests*, *13*(10), 1739. https://doi.org/10.3390/f13101739
35. Hou, X., Gao, Y., Liu, X., Xu, T., Xu, J., Zhao, Y., Liu, Y. (2025). Experimental study on the pore structure and permeability characteristics of clay soil under freezing–thawing cycles. *Scientific Reports*, *15*(1), 31216. https://doi.org/10.1038/s41598-025-15870-4
36. Islam, R., Ahmed, R., Dey, B., Haque, Md. S., Aktar, S., Bhuiyan, M. S., Arif, M. S., Habib Ador, Md. A., Ul Haque, M. M., Saha, N. (2023). Salinity hazard drives the alteration of occupation, land use and ecosystem service in the coastal areas: Evidence from the south-western coastal region of Bangladesh. *Heliyon*, *9*(8), e18512. https://doi.org/10.1016/j.heliyon.2023.e18512
37. James, K., Macreadie, P. I., Burdett, H. L., Davies, I., Kamenos, N. A. (2024). It's time to broaden what we consider a 'blue carbon ecosystem.' *Global Change Biology*, *30*(5), e17261. https://doi.org/10.1111/gcb.17261
38. Jha, A., Bonetti, S., Smith, A. P., Souza, R., Calabrese, S. (2023). Linking soil structure, hydraulic properties, and organic carbon dynamics: A holistic framework to study the impact of climate change and land management. *Journal of Geophysical Research: Biogeosciences*, *128*(7), e2023JG007389. https://doi.org/10.1029/2023JG007389
39. Kaden, U. S., Schmid, S., Vieweg, M., Scholz, M., Dufour, S. (2026). European riverine and coastal wetlands under pressure: Biodiversity and climate change. *Nature Conservation*, *62*, 13–45. https://doi.org/10.3897/natureconservation.62.163636
40. Kaushal, S. S., Likens, G. E., Pace, M. L., Reimer, J. E., Maas, C. M., Galella, J. G., Utz, R. M., Duan, S., Kryger, J. R., Yaculak, A. M., Boger, W. L., Bailey, N. W., Haq, S., Wood, K. L., Wessel, B. M., Park, C. E., Collison, D. C., Aisin, B. Y. 'aaqob I., Gedeon, T. M., … Woglo, S. A. (2021). Freshwater salinization syndrome: From emerging global problem to managing risks. *Biogeochemistry*, *154*(2), 255–292. https://doi.org/10.1007/s10533-021-00784-w
41. Kunselman, A. R. (2024). A brief overview of pilot studies and their sample size justification. *Fertility and Sterility*, *121*(6), 899–901. https://doi.org/10.1016/j.fertnstert.2024.01.040
42. Kurek, M. R., Wickland, K. P., Nichols, N. A., McKenna, A. M., Anderson, S. M., Dornblaser, M. M., Koupaei-Abyazani, N., Poulin, B. A., Bansal, S., Fellman, J. B., Druschel, G. K., Bernhardt, E. S., Spencer, R. G. M. (2024). Linking dissolved organic matter composition to landscape properties in wetlands across the United States of America. *Global Biogeochemical Cycles*, *38*(5), e2023GB007917. https://doi.org/10.1029/2023GB007917
43. Leon, A. C., Davis, L. L., Kraemer, H. C. (2011). The role and interpretation of pilot studies in clinical research. *Journal of Psychiatric Research*, *45*(5), 626–629. https://doi.org/10.1016/j.jpsychires.2010.10.008
44. Li, X., Bellerby, R., Craft, C., Widney, S. E. (2018). Coastal wetland loss, consequences, and challenges for restoration. *Anthropocene Coasts*, *1*(1), 1–15. https://doi.org/10.1139/anc-2017-0001
45. Lin, S., Zhou, Y., Wang, W., Sardans, J., Li, Y., Fu, C., Zeng, F., Song, Z., Tariq, A., Peñuelas, J. (2024). Losses and destabilization of soil organic carbon stocks in coastal wetlands converted into aquaculture ponds. *Global Change Biology*, *30*(9), e17480. https://doi.org/10.1111/gcb.17480

46. Liu, Z.-K., Zhang, L., Jin, S., Yu, H., He, J.-Z., Shen, J.-P. (2025). Land use changes alter microbial functional gene diversity and its relationship with soil ecosystem multifunctionality in a subtropical estuary. *Frontiers in Microbiology*, *16*, 1592901. https://doi.org/10.3389/fmicb.2025.1592901
47. MacFarland, T. W., Yates, J. M. (2016). Kruskal–Wallis H-Test for Oneway Analysis of Variance (ANOVA) by Ranks. In T. W. MacFarland & J. M. Yates, *Introduction to Nonparametric Statistics for the Biological Sciences Using R* (pp. 177–211). Springer International Publishing. https://doi.org/10.1007/978-3-319-30634-6_6
48. Marchand, C., Baltzer, F., Lallier-Vergès, E., Albéric, P. (2004). Pore-water chemistry in mangrove sediments: Relationship with species composition and developmental stages (French Guiana). *Marine Geology*, *208*(2–4), 361–381. https://doi.org/10.1016/j.margeo.2004.04.015
49. McKight, P. E., Najab, J. (2010). Kruskal-Wallis Test. In I. B. Weiner & W. E. Craighead (Eds.), *The Corsini Encyclopedia of Psychology* (1st ed., pp. 1–1). Wiley. https://doi.org/10.1002/9780470479216.corpsy0491
50. Meurer, K. H. E., Chenu, C., Coucheney, E., Herrmann, A. M., Keller, T., Kätterer, T., Nimblad Svensson, D., Jarvis, N. (2020). *Modelling dynamic interactions between soil structure and the storage and turnover of soil organic matter*. Biogeochemistry: Soils. https://doi.org/10.5194/bg-2020-135
51. Newton, A., Icely, J., Cristina, S., Perillo, G. M. E., Turner, R. E., Ashan, D., Cragg, S., Luo, Y., Tu, C., Li, Y., Zhang, H., Ramesh, R., Forbes, D. L., Solidoro, C., Béjaoui, B., Gao, S., Pastres, R., Kelsey, H., Taillie, D., … Kuenzer, C. (2020). Anthropogenic, direct pressures on coastal wetlands. *Frontiers in Ecology and Evolution*, *8*, 144. https://doi.org/10.3389/fevo.2020.00144
52. O'Kelly, B. C. (2017). Measurement, interpretation and recommended use of laboratory strength properties of fibrous peat. *Geotechnical Research*, *4*(3), 136–171. https://doi.org/10.1680/jgere.17.00006
53. Okovido, J. O., Obroku, E. O. (2021). Study of density and void ratio relation for reconstituted tropical residual soil at varying fines contents. *Nigerian Journal of Technology*, *40*(3), 371–378. https://doi.org/10.4314/njt.v40i3.3
54. Ostertagová, E., Ostertag, O., Kováč, J. (2014). Methodology and application of the Kruskal-Wallis Test. *Applied Mechanics and Materials*, *611*, 115–120. https://doi.org/10.4028/www.scientific.net/AMM.611.115
55. Piñeiro-Juncal, N., Mateo, M. Á., Leiva-Dueñas, C., Serrano, E., Inostroza, K., Soler, M., Apostolaki, E. T., Lavery, P., Duarte, C. M., Lafratta, A., Serrano, O. (2025). Soil organic carbon depth profiles and centennial and millennial decay rates in tidal marsh, mangrove and seagrass blue carbon ecosystems. *Communications Earth & Environment*, *6*(1), 504. https://doi.org/10.1038/s43247-025-02390-2
56. Prasad, R. (2021). Assessing anthropogenic impacts in coastal areas through land use and land cover changes from 1980 to 2019 using remote sensing and GIS techniques: A case study of Southern Coastal Gujarat, India. *YES Congress, Deutsches GeoForschungsZentrum*, 69–73. https://doi.org/10.2312/YES19.05
57. Rabbi, S. M. F., Warren, C. R., Swarbrick, B., Minasny, B., McBratney, A. B., Young, I. M. (2024). Microbial decomposition of organic matter and wetting–drying promotes aggregation in artificial soil but porosity increases only in wet-dry condition. *Geoderma*, *447*, 116924. https://doi.org/10.1016/j.geoderma.2024.116924
58. Rimba, A. B., Atmaja, T., Mohan, G., Chapagain, S. K., Arumansawang, A., Payus, C., Fukushi, K. (2020). Identifying Land Use and Land Cover (LULC) Change From 2000 to 2025 Driven by Tourism Growth: A Study Case in Bali. *The International Archives of the Photogrammetry, Remote Sensing and Spatial Information Sciences*, *XLIII-B3-2020*, 1621–1627. https://doi.org/10.5194/isprs-archives-XLIII-B3-2020-1621-2020
59. Roberts, A., Roche, M., Sainani, K. L. (2023). Exploratory analyses: How to meaningfully interpret and report them. *PM&R*, *15*(6), 800–804. https://doi.org/10.1002/pmrj.12980
60. Rühlmann, J., Körschens, M., Graefe, J. (2006). A new approach to calculate the particle density of soils considering properties of the soil organic matter and the mineral matrix. *Geoderma*, *130*(3–4), 272–283. https://doi.org/10.1016/j.geoderma.2005.01.024
61. Saengsupavanich, C., Agarwala, N., Magdalena, I., Ratnayake, A. S., Ferren, V. (2024). Impacts of a growing population on the coastal environment of the Bay of Bengal. *Anthropocene Coasts*, *7*(1), 24. https://doi.org/10.1007/s44218-024-00055-9
62. Skempton, A. W., Petley, D. J. (1970). Ignition loss and other properties of peats and clays from Avon mouth, King's Lynn and Cranberry Moss. *Géotechnique*, *20*(4), 343–356. https://doi.org/10.1680/geot.1970.20.4.343
63. Stagg, C. L., Schoolmaster, D. R., Krauss, K. W., Cormier, N., Conner, W. H. (2017). Causal mechanisms of soil organic matter decomposition: Deconstructing salinity and flooding impacts in coastal wetlands. *Ecology*, *98*(8), 2003–2018. https://doi.org/10.1002/ecy.1890
64. Sunarta, I. N., Saifulloh, M. (2022). Coastal tourism: Impact for built-up area growth and correlation to vegetation and water indices derived from Sentinel-2 remote sensing imagery. *GeoJournal of Tourism and Geosites*, *41*(2), 509–516. https://doi.

org/10.30892/gtg.41223-857

65. Tang, C.-S., Cheng, Q., Gong, X., Shi, B., Inyang, H. I. (2023). Investigation on microstructure evolution of clayey soils: A review focusing on wetting/drying process. *Journal of Rock Mechanics and Geotechnical Engineering*, *15*(1), 269–284. https://doi.org/10.1016/j.jrmge.2022.02.004
66. Temmerman, S., Horstman, E. M., Krauss, K. W., Mullarney, J. C., Pelckmans, I., Schoutens, K. (2023). Marshes and mangroves as nature-based coastal storm buffers. *Annual Review of Marine Science*, *15*(1), 95–118. https://doi.org/10.1146/annurev-marine-040422-092951
67. Van Bijsterveldt, C. E. J., Van Wesenbeeck, B. K., Van Der Wal, D., Afiati, N., Pribadi, R., Brown, B., Bouma, T. J. (2020). How to restore mangroves for greenbelt creation along eroding coasts with abandoned aquaculture ponds. *Estuarine, Coastal and Shelf Science*, *235*, 106576. https://doi.org/10.1016/j.ecss.2019.106576
68. Van Wesenbeeck, B. K., Balke, T., Van Eijk, P., Tonneijck, F., Siry, H. Y., Rudianto, M. E., Winterwerp, J. C. (2015). Aquaculture induced erosion of tropical coastlines throws coastal communities back into poverty. *Ocean & Coastal Management*, *116*, 466–469. https://doi.org/10.1016/j.ocecoaman.2015.09.004
69. Vo Ai Mi, N. (2023). Roadway settlement characteristics on Mekong delta for various landforms. *International Journal of GEOMATE*, *25*(111). https://doi.org/10.21660/2023.111.4006
70. Wang, S., Feng, Q., Zhou, Y., Mao, X., Chen, Y., Xu, H. (2017). Dynamic changes in water and salinity in saline-alkali soils after simulated irrigation and leaching. *PLOS ONE*, *12*(11), e0187536. https://doi.org/10.1371/journal.pone.0187536
71. Wei, Y., Tang, C.-S., Zhu, C., Cheng, Q., Lu, Y., Li, L., Tian, B.-G., Shi, B. (2024). Influence of desiccation during freeze-thaw cycles on volumetric shrinkage and tensile strength of compacted clayey soils. *Engineering Geology*, *334*, 107513. https://doi.org/10.1016/j.enggeo.2024.107513
72. White, E., Kaplan, D. (2017). Restore or retreat? Saltwater intrusion and water management in coastal wetlands. *Ecosystem Health and Sustainability*, *3*(1), e01258. https://doi.org/10.1002/ehs2.1258
73. Widantara, K. W., Mutaqin, B. W. (2024). Multi-hazard assessment in the coastal tourism city of Denpasar, Bali, Indonesia. *Natural Hazards*, *120*(8), 7105–7138. https://doi.org/10.1007/s11069-024-06506-3
74. Xia, S., Song, Z., Van Zwieten, L., Guo, L., Yu, C., Wang, W., Li, Q., Hartley, I. P., Yang, Y., Liu, H., Wang, Y., Ran, X., Liu, C., Wang, H. (2022). Storage, patterns and influencing factors for soil organic carbon in coastal wetlands of China. *Global Change Biology*, *28*(20), 6065–6085. https://doi.org/10.1111/gcb.16325
75. Xin, P., Wilson, A., Shen, C., Ge, Z., Moffett, K. B., Santos, I. R., Chen, X., Xu, X., Yau, Y. Y. Y., Moore, W., Li, L., Barry, D. A. (2022). Surface water and groundwater interactions in salt marshes and their impact on plant ecology and coastal biogeochemistry. *Reviews of Geophysics*, *60*(1), e2021RG000740. https://doi.org/10.1029/2021RG000740
76. Yang, Y., Wang, W., Hu, Q., Yao, X., Yang, W., Wen, S., Wu, H., Jin, J., Shen, L. (2025). Conversion of coastal wetlands to paddy fields substantially decreases methane oxidation potential and methanotrophic abundance on the eastern coast of China. *Water Research*, *272*, 122962. https://doi.org/10.1016/j.watres.2024.122962
77. Zhang, R., Liu, L., Yang, Y., Xu, S., He, Z., Tracy, M. E., Shi, S., Guo, Z. (2025). Seawater tides shaped mangrove sediment a bacterial community drastically distinct from supratidal land soil. *BMC Microbiology*, *25*(1), 742. https://doi.org/10.1186/s12866-025-04486-3
78. Zhang, Y., Li, X., Šimůnek, J., Shi, H., Chen, N., Hu, Q., Tian, T. (2021). Evaluating soil salt dynamics in a field drip-irrigated with brackish water and leached with freshwater during different crop growth stages. *Agricultural Water Management*, *244*, 106601. https://doi.org/10.1016/j.agwat.2020.106601
79. Zhao, D., Dong, J., Ji, S., Huang, M., Quan, Q., Liu, J. (2020). Effects of contemporary land use types and conversions from wetland to paddy field or dry land on soil organic carbon fractions. *Sustainability*, *12*(5), 2094. https://doi.org/10.3390/su12052094
80. Zhao, Z., Feng, X., Liu, C., Han, Y., Long, G., Chen, S., Lin, Q., Gong, J., Shen, Y., Mao, Z., Sounilan, T., Zhang, X., Li, L., Pan, G. (2024). Soil organic carbon storage, microbial abundance and pore structure characteristics of macroaggregates across a soil-landscape sequence in a subtropical hilly watershed. *CATENA*, *242*, 108056. https://doi.org/10.1016/j.catena.2024.108056
81. Zhu, B., Salazar, D., Willems, P. (2024). Impacts of external factors in salinity patterns via numerical modeling along the Scheldt Estuary, Belgium. *Journal of Hydrology: Regional Studies*, *56*, 102026. https://doi.org/10.1016/j.ejrh.2024.102026